

## Research Article

# Nonlinear Dynamic Analysis on the Rain-Wind-Induced Vibration of Cable Considering the Equilibrium Position of Rivulet

Xijun Liu,<sup>1,2</sup> Bing Huo,<sup>1,2</sup> and Suxia Zhang<sup>1,2</sup>

<sup>1</sup> Department of Mechanics, School of Mechanical Engineering, Tianjin University, Tianjin 300072, China

<sup>2</sup> Tianjin Key Laboratory of Nonlinear Dynamics and Chaos Control, Tianjin 300072, China

Correspondence should be addressed to Bing Huo; [huobing@tju.edu.cn](mailto:huobing@tju.edu.cn)

Received 1 October 2013; Accepted 19 November 2013

Academic Editor: Massimiliano Ferrara

Copyright © 2013 Xijun Liu et al. This is an open access article distributed under the Creative Commons Attribution License, which permits unrestricted use, distribution, and reproduction in any medium, provided the original work is properly cited.

The nonlinear dynamic behavior of rain-wind-induced vibration of inclined cable is investigated with the consideration of the equilibrium position of the moving rivulet. The partial differential governing equations of three-degree-of-freedom on the model of rain-wind-induced cable vibration are established, which are proposed for describing the nonlinear interactions among the in-plane, out-of-plane vibration of the cable and the oscillation of the moving rivulet. The Galerkin method is applied to discretize the partial differential governing equations. The approximately analytic solution is obtained by using the method of averaging. The unique correspondence between the wind and the equilibrium position of the rivulet is ascertained. The presence of rivulet at certain positions on the surface of cable is then proved to be one of the trigger for wind-rain-induced cable vibration. The nonlinear dynamic phenomena of the inclined cable subjected to wind and rain turbulence are then studied by varying the parameters including mean wind velocity, Coulomb damping force, damping ratio, the span length, and the initial tension of the inclined cable on the model. The jump phenomenon is also observed which occurs when there are multiple solutions in the system.

## 1. Introduction

Dynamic behavior of corresponding differential systems has been of extensive concern and investigated by many scholars [1–8]. One of the systems is the inclined cable, which is a structure characterized by small stiffness, low mass, and light damping. The similar structures including transmission line, suspended cable, and submarine cable are widely used in the long-span structures, so the dynamic study of the inclined cable is of great engineering significance. Rain-wind-induced vibration of inclined cable is a phenomenon of large amplitude vibration with low frequency under the conditions of rain and wind. Many wind tunnel tests have been carried on a cable model. Large amplitude vibrations of cables were first observed by Hikami and Shiraishi [9]. Upper rivulet was regarded as the origin of large amplitude vibration due to its formulation on the cable, causing the cable cross section aerodynamically unstable. Yamaguchi [10] took the lead in aerodynamic test of cable with artificial rivulet. Aerodynamic

forces acting on the cable were obtained. Matsumoto et al. [11] reported that another factor named an axial flow generated at the near wake of the inclined cable may trigger the rain-wind-induced oscillations. He stated that rain-wind-induced vibration can be explained as a vortex-induced vibration, which occurs at limited high reduced wind velocity region [12]. Bosdogianni and Olivari [13] compared wind tunnel results of cables with moving rivulet and fixed rivulet. They concluded that it was the presence of rivulet at certain positions on the surface of cable and not the motion of rivulet that caused cable instability. Then the aerodynamic forces acting on the moving rivulet were first measured by Gu et al. [14], proposing a new description of friction force between the water rivulet and the cable surface.

On the basis of the measured aerodynamic coefficients, the kinetic equations of rain-wind-induced vibration have been established. However, before the measurement of the aerodynamic coefficients on the moving rivulet, the motion of rivulet was assumed to be harmonic [15–17]. With the

acquisition of the aerodynamic coefficients on the moving rivulet, the analytic model for cable with the kinetic equation of the rivulet was built [18]. Zhang et al. [3] presented a two-degree-of-freedom model of the rain-wind-induced vibration of a continuous stay cable. The phenomenon of bifurcation was observed in the system using the singularity theory. Zhang et al. [19] established the three-degree-of-freedom model of rain-wind-induced vibration of inclined cable. The motion characteristics of rivulet were achieved with two rivulet models through numerical calculation and some more rational explanations of the phenomenon were obtained.

The influences of equilibrium position of rivulet on cable have been studied, in which the equilibrium position of rivulet was always assumed to be independent of wind. The equilibrium position of rivulet was altered factitiously to inspect its effects on the vibration while the mean wind velocity was fixed [15, 18]. However, the equilibrium position of rivulet is uniquely corresponding to the wind once the mass of the rivulet is fixed. Meanwhile, the similar structures including beam, suspended cables, and inclined cable without wind or rain have been extensively researched analytically to discover more dynamic phenomena [4–8]. However, the nonlinear dynamic behavior of rain-wind-induced vibration has been rarely investigated using approximately analytic method for its complexity.

In comparison with the literature above, the equilibrium position of the moving rivulet is considered and the nonlinear dynamic characteristics of rain-wind-induced vibration are investigated analytically by using the approximate method of averaging. The present paper established the continuum model of the inclined cable subjected to wind and rain turbulence with the consideration of the equilibrium position of the rivulet. The reliance of the equilibrium position of the rivulet on wind is figured out and the effects of the equilibrium position of the rivulet on the cable vibration are observed and proved. Furthermore, the amplitude response curves of parameters including mean wind velocity, Coulomb damping force, damping ratio, the span length, and the initial tension of the inclined cable present abundant dynamic behaviors. The jump phenomenon is also observed when multivalued solutions exit in the system.

## 2. Model and Nonlinear Equations

Assumptions of inclined cable are made in present paper: (1) The flexural rigidity, torsional stiffness and shear stiffness are ignored; (2) The constitutive relation of cable deformation submits to Hooke's law and the points bear the stress evenly; (3) The axial motion of the cable is ignored; (4) The influences of bridge and tower are disregarded.

The analytic model of rain-wind-induced vibration of inclined cable is shown in Figures 1(a), 1(b), and 1(c),  $U_0$  is mean wind velocity,  $\alpha$  is cable angle,  $\beta$  is wind angle,  $L$  is the span length of the cable, and  $v$  and  $w$  are dynamic displacement in the  $y$  and  $z$  direction, respectively.  $v_0$  is deflection at the equilibrium position of cable. Define that the vibration in the plane  $x$ - $y$  is in-plane vibration, while the

vibration in the plane  $x$ - $y$  is out-of-plane vibration.  $M$  is the mass per unit length of cable,  $T$  is the initial tension of the cable, and  $\tau$  is the dynamic tension of the cable.  $ds$  and  $ds_0$  are arc length of undeformed and deformed cable, respectively.

Figure 1(d) presents the force analysis of rivulet.  $\theta_0$  is the equilibrium position of rivulet,  $\theta$  is dynamic displacement of rivulet which is the angle deviating from the equilibrium position,  $\varphi$  is dynamic displacement of rivulet which is the angle deviating from  $y$  direction.  $m$  is the mass per unit length of rivulet,  $g$  is the gravity acceleration,  $R$  is the radius of cable,  $F_0$  is Coulomb damping force whose direction is opposite to its motion,  $\zeta_r$  is the linear viscous damping coefficient between cable and rivulet, and effective angle of attack  $\gamma$  is the angle between effective wind velocity  $U$  and  $z$  direction.  $\psi$  is the angle between relative wind velocity  $U_r$  and  $z$  direction.

Balance equations of the system are obtained from the force analysis of the cable element and rivulet (see Figures 1(c) and 1(d)):

$$\begin{aligned} M \frac{\partial^2 v}{\partial t^2} &= \frac{\partial}{\partial s} \left[ (T + \tau) \left( \frac{\partial v}{\partial s} + \frac{dv_0}{ds} \right) \right] - \zeta_v \frac{\partial v}{\partial t} + Mg \cos \alpha + F_y, \\ M \frac{\partial^2 w}{\partial t^2} &= \frac{\partial}{\partial s} \left[ (T + \tau) \left( \frac{\partial w}{\partial s} \right) \right] - \zeta_w \frac{\partial w}{\partial t} + F_z, \\ mR\ddot{\varphi} &= mg \cos \alpha \sin \varphi - F_0 \frac{\dot{\varphi}}{|\dot{\varphi}|} - \zeta_r R \dot{\varphi}, \\ &\quad - f_\tau + m\ddot{w} \cos \varphi - m\ddot{v} \sin \varphi, \end{aligned} \quad (1)$$

where

$$\begin{aligned} \tau &= EA \cdot \varepsilon_0, \quad \varepsilon_0 \approx \frac{ds^2 - ds_0^2}{2 \cdot ds_0^2}, \\ ds_0 &= \sqrt{1 + v_{0x}^2} dx, \quad ds = \sqrt{1 + (v_{0x} + v_x)^2 + w_x^2} dx, \quad (2) \\ v_0 &= \frac{MgL \cos \alpha}{2T} \left( x - \frac{x^2}{L} \right). \end{aligned}$$

$E$  is the elasticity modulus of cable,  $A$  is the cross sectional area of cable, and  $\varepsilon_0$  is dynamic strain.  $\zeta_v$ ,  $\zeta_w$  are the damping coefficients of in-plane and out-of-plane vibration, respectively.  $F_y$ ,  $F_z$ , and  $f_\tau$  are the aerodynamic forces on the in-plane, out-of-plane, and rivulet vibration, respectively, with the function of  $\dot{v}$ ,  $\dot{w}$ ,  $\dot{\varphi}$ , and  $\varphi$  which are defined by

$$\begin{aligned} F_y &= -\frac{\rho D U_r^2}{2} [C_L(\psi^*) \cos \varphi + C_D(\psi^*) \sin \varphi], \\ F_z &= \frac{\rho D U_r^2}{2} [C_D(\psi^*) \cos \varphi + C_L(\psi^*) \sin \varphi], \quad (3) \\ f_\tau &= \frac{\rho B U_r^2}{2} [-c_x(\varphi) \cos \varphi + c_y(\varphi) \sin \varphi], \end{aligned}$$

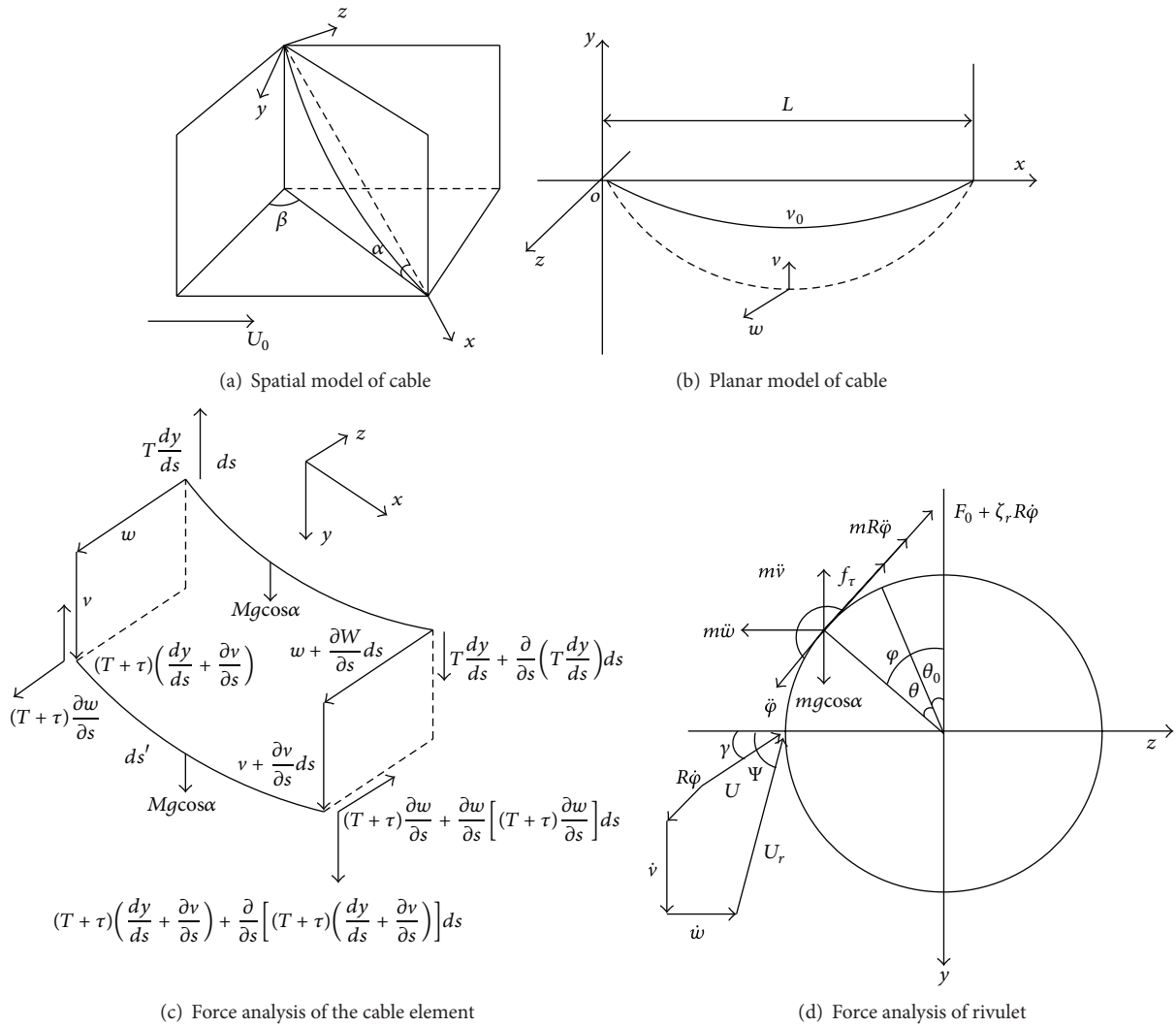


FIGURE 1: Mechanical model of inclined cable.

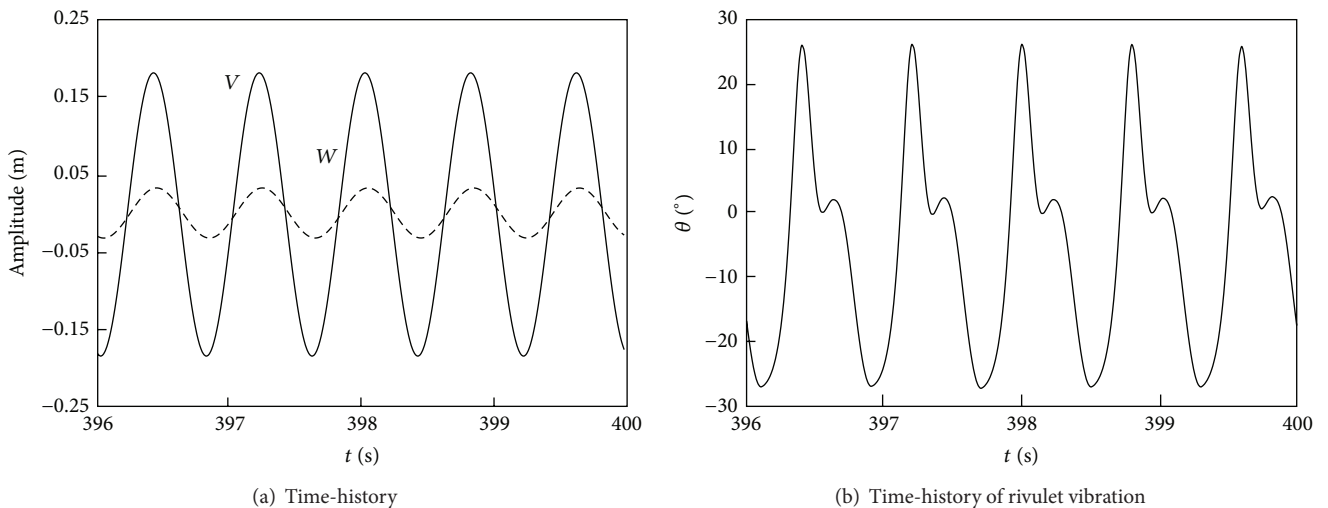


FIGURE 2: Displacements of in-plane and out-of-plane vibration.

where  $\rho$  is air density,  $D$  is the diameter of the cable,  $B$  is the characteristic length of rivulet, and  $\psi^*$  is equivalent wind attack angle and can be written as

$$\begin{aligned}\psi^* &= \psi - \varphi, \\ \psi &= \tan^{-1} \frac{U \sin \gamma + \dot{v} + R\dot{\varphi} \sin \varphi}{U \cos \gamma - \dot{w} + R\dot{\varphi} \cos \varphi}, \\ \gamma &= \sin^{-1} \left( \frac{\sin \alpha \sin \beta}{\sqrt{\cos^2 \alpha + \sin^2 \alpha \sin^2 \beta}} \right),\end{aligned}$$

$$U_r = \sqrt{(U \cos \gamma + R\dot{\varphi} \cos \varphi - \dot{w})^2 + (U \sin \gamma + \dot{v} + R\dot{\varphi} \sin \varphi)^2},$$

$$U = U_0 \sqrt{\cos^2 \beta + \sin^2 \alpha \sin^2 \beta} = U_0 \sqrt{\sin^2 \alpha + \cos^2 \alpha \cos^2 \beta}. \quad (4)$$

In (3), lift coefficient  $C_L$ , resistance coefficient  $C_D$  of cable are the fitting functions of  $\psi^*$ , aerodynamic coefficients of rivulet  $c_x$  and  $c_y$  are the fitting functions of  $\varphi$  which are obtained in the experiment [18] and can be expressed as

$$\begin{aligned}C_L(\psi^*) &= e_{11} + e_{12}\psi^* + e_{13}\psi^{*2} + e_{14}\psi^{*3}, \\ C_D(\psi^*) &= e_{21} + e_{22}\psi^* + e_{23}\psi^{*2} + e_{24}\psi^{*3}, \\ c_x(\varphi) &= e_{31} + e_{32}\varphi + e_{33}\varphi^2 + e_{34}\varphi^3, \\ c_y(\varphi) &= e_{41} + e_{42}\varphi + e_{43}\varphi^2 + e_{44}\varphi^3,\end{aligned} \quad (5)$$

where  $e_{ij}$  are constant coefficients,  $i = 1 \sim 4$ ,  $j = 1 \sim 4$ . At static situation, the force analysis of rivulet is given by

$$mg \cos \alpha \sin \varphi = f_\tau(\dot{v}, \dot{w}, \varphi, \dot{\varphi})_{\dot{v}=0, \dot{w}=0, \dot{\varphi}=0}. \quad (6)$$

The equilibrium position  $\theta_0$  can be attained from (6) and expressed as  $\theta_0 = \Theta(U_0, m)$ . The equation of rivulet on the equilibrium position is obtained by substituting  $\varphi = \theta + \theta_0$  (Figure 1(d)) into system (1). Galerkin method is then adopted to discretize system (1) and the first mode of vibration is reserved, assuming that

$$\begin{aligned}v &= V(t) \sin\left(\frac{\pi x}{L}\right), \\ w &= W(t) \sin\left(\frac{\pi x}{L}\right)\end{aligned} \quad (7)$$

the final equations are obtained:

$$\begin{aligned}\ddot{V} + \omega_v V + \zeta_v \dot{V} &= g_{v1} V^2 + g_{v2} W^2 + g_{v3} V W^2 \\ &+ g_{v4} V^3 + F_v(V, \dot{V}, W, \dot{W}, \theta, \dot{\theta}), \\ \ddot{W} + \omega_w W + \zeta_w \dot{W} &= g_{w1} V W + g_{w2} W^3 \\ &+ g_{w3} V^2 W + F_w(V, \dot{V}, W, \dot{W}, \theta, \dot{\theta}), \\ \ddot{\theta} + \omega_\theta \theta + \zeta_\theta \dot{\theta} &= g_{\theta1} V^2 + g_{\theta2} W^2 + g_{\theta3} V \theta \\ &+ g_{\theta4} W \theta + g_{\theta5} V W \theta + g_{\theta6} V W^2 \\ &+ g_{\theta7} V \theta^2 + g_{\theta8} W \theta^2 + g_{\theta9} V^2 \theta \\ &+ g_{\theta10} W^2 \theta + g_{\theta11} V^3 + g_{\theta12} W^3 \\ &+ g_{\theta13} V^2 W + g_{\theta14} V W \\ &+ g_{\theta15} V W^2 + g_{\theta16} F_0 \operatorname{sgn}(\dot{\theta}) \\ &+ F_\theta(V, \dot{V}, W, \dot{W}, \theta, \dot{\theta}),\end{aligned} \quad (8)$$

where

$$\begin{aligned}F_i(V, \dot{V}, W, \dot{W}, \theta, \dot{\theta}) &= a_{i1} \dot{V} + a_{i2} \dot{W} + a_{i3} \theta + a_{i4} \dot{V}^2 \\ &+ a_{i5} \dot{W}^2 + a_{i6} \theta^2 + a_{i7} \dot{\theta}^2 + a_{i8} \dot{V} \dot{W} \\ &+ a_{i9} \dot{V} \theta + a_{i10} \dot{V} \dot{\theta} + a_{i11} \dot{W} \theta \\ &+ a_{i12} \dot{W} \dot{\theta} + a_{i13} \theta \dot{\theta} + a_{i14} \dot{V} \dot{W} \theta \\ &+ a_{i15} \dot{V} \dot{W} \dot{\theta} + a_{i16} \dot{V} \theta \dot{\theta} + a_{i17} \dot{W} \theta \dot{\theta} \\ &+ a_{i18} \dot{V} \dot{W}^2 + a_{i19} \dot{V} \theta^2 + a_{i20} \dot{V} \dot{\theta}^2 \\ &+ a_{i21} \dot{V}^2 \dot{W} + a_{i22} \dot{W} \theta^2 + a_{i23} \dot{W} \dot{\theta}^2 \\ &+ a_{i24} \dot{V}^2 \theta + a_{i25} \dot{W}^2 \theta + a_{i26} \theta \dot{\theta}^2 \\ &+ a_{i27} \dot{V}^2 \dot{\theta} + a_{i28} \dot{W}^2 \dot{\theta} + a_{i29} \theta^2 \dot{\theta} \\ &+ a_{i30} \dot{V}^3 + a_{i31} \dot{W}^3 + a_{i32} \dot{\theta}^3.\end{aligned} \quad (9)$$

$\omega_i$  is the natural frequency of in-plane, out-of-plane, and rivulet vibration, respectively.  $a_{i1} \sim a_{i32}$ ,  $g_{i1} \sim g_{i16}$  are integral constants related to physical parameters of cable and mean wind velocity,  $i = v, w, \theta$ . The equations are composed of geometric nonlinearity and aerodynamic nonlinearity.

### 3. Average Analysis

Nondimensionalize system (8) and assume that  $V = x_1$ ,  $\dot{V} = x_2$ ,  $W = x_3$ ,  $\dot{W} = x_4$ ,  $\theta = x_5$ , and  $\dot{\theta} = x_6$ ; then system (8) becomes

$$\begin{aligned} \dot{x}_1 &= x_2, \\ \dot{x}_2 &= a_1x_1 + a_2x_5 + \varepsilon F_1(x_1, x_2, x_3, x_4, x_5, x_6), \\ \dot{x}_3 &= x_4, \\ \dot{x}_4 &= b_1x_3 + b_2x_5 + \varepsilon F_2(x_1, x_2, x_3, x_4, x_5, x_6), \\ \dot{x}_5 &= x_6, \end{aligned} \tag{10}$$

$$\begin{aligned} \dot{x}_6 &= c_1x_1 + c_2x_3 + c_3x_5 \\ &+ \varepsilon F_3(x_1, x_2, x_3, x_4, x_5, x_6) + c_{50}F_0 \operatorname{sgn}(x_6), \\ F_1 &= a_3x_2 + a_4x_4 + a_5x_6 + a_6x_1^2 + a_7x_2^2 + a_8x_3^2 + a_9x_4^2 \\ &+ a_{10}x_5^2 + a_{11}x_6^2 + a_{12}x_2x_4 + a_{13}x_2x_5 + a_{14}x_2x_6 \\ &+ a_{15}x_4x_5 + a_{16}x_4x_6 + a_{17}x_5x_6 + a_{18}x_2x_4x_5 \\ &+ a_{19}x_2x_4x_6 + a_{20}x_2x_5x_6 + a_{21}x_4x_5x_6 + a_{22}x_2x_4^2 \\ &+ a_{23}x_2x_5^2 + a_{24}x_2x_6^2 + a_{25}x_4x_2^2 + a_{26}x_4x_5^2 \\ &+ a_{27}x_4x_6^2 + a_{28}x_5x_2^2 + a_{29}x_5x_4^2 + a_{30}x_5x_6^2 \\ &+ a_{31}x_6x_2^2 + a_{32}x_6x_4^2 + a_{33}x_6x_5^2 + a_{34}x_1x_3^2 \\ &+ a_{35}x_1^3 + a_{36}x_2^3 + a_{37}x_4^3 + a_{38}x_6^3, \end{aligned}$$

$$\begin{aligned} F_2 &= b_3x_2 + b_4x_4 + b_5x_6 + b_6x_2^2 + b_7x_4^2 + b_8x_5^2 + b_9x_6^2 \\ &+ b_{10}x_1x_3 + b_{11}x_2x_4 + b_{12}x_2x_5 + b_{13}x_2x_6 \\ &+ b_{14}x_4x_5 + b_{15}x_4x_6 + b_{16}x_5x_6 + b_{17}x_2x_4x_5 \\ &+ b_{18}x_2x_4x_6 + b_{19}x_2x_5x_6 + b_{20}x_4x_5x_6 + b_{21}x_2x_4^2 \\ &+ b_{22}x_2x_5^2 + b_{23}x_2x_6^2 + b_{24}x_3x_1^2 + b_{25}x_4x_2^2 \\ &+ b_{26}x_4x_5^2 + b_{27}x_4x_6^2 + b_{28}x_5x_2^2 + b_{29}x_5x_4^2 \\ &+ b_{30}x_5x_6^2 + b_{31}x_6x_2^2 + b_{32}x_6x_4^2 + b_{33}x_6x_5^2 \\ &+ b_{34}x_1x_3^2 + b_{35}x_2^3 + b_{36}x_4^3 + b_{37}x_6^3, \end{aligned}$$

$$\begin{aligned} F_3 &= c_4x_2 + c_5x_4 + c_6x_6 + c_7x_1^2 + c_8x_2^2 + c_9x_3^2 + c_{10}x_4^2 \\ &+ c_{11}x_5^2 + c_{12}x_6^2 + c_{13}x_1x_3 + c_{14}x_1x_5 + c_{15}x_2x_4 \\ &+ c_{16}x_2x_5 + c_{17}x_2x_6 + c_{18}x_3x_5 + c_{19}x_4x_5 + c_{20}x_4x_6 \\ &+ c_{21}x_5x_6 + c_{22}x_1x_3x_5 + c_{23}x_2x_4x_5 + c_{24}x_2x_4x_6 \\ &+ c_{25}x_2x_5x_6 + c_{26}x_4x_5x_6 + c_{27}x_1x_3^2 + c_{28}x_1x_5^2 \\ &+ c_{29}x_2x_4^2 + c_{30}x_2x_5^2 + c_{31}x_2x_6^2 + c_{32}x_3x_1^2 + c_{33}x_3x_5^2 \end{aligned}$$

$$\begin{aligned} &+ c_{34}x_4x_2^2 + c_{35}x_4x_5^2 + c_{36}x_4x_6^2 + c_{37}x_5x_1^2 + c_{38}x_5x_2^2 \\ &+ c_{39}x_5x_3^2 + c_{40}x_5x_4^2 + c_{41}x_5x_6^2 + c_{42}x_6x_2^2 \\ &+ c_{43}x_6x_4^2 + c_{44}x_6x_5^2 + c_{45}x_1^3 + c_{46}x_2^3 \\ &+ c_{47}x_3^3 + c_{48}x_4^3 + c_{49}x_6^3. \end{aligned} \tag{11}$$

$a_1 \sim a_{38}$ ,  $b_1 \sim b_{37}$ , and  $c_1 \sim c_{50}$  are integral constants. The analytic solutions are assumed to be

$$x_s = \sum_{k=1}^3 A_k \phi_{sk}(\theta_k). \tag{12}$$

$A_k(t)$  is amplitude and  $\theta_k(t)$  is phase position. They can be obtained according to the orthogonality of derived equations and conjugate equations which are given by

$$\frac{dA_k}{dt} = \frac{\varepsilon}{\Delta_k} \sum_{s=1}^6 F_s \psi_{sk}(\theta_k), \tag{13}$$

$$\frac{d\theta_k}{dt} = \lambda_k - \frac{\varepsilon}{\Delta_k A_k} \sum_{s=1}^6 F_s \psi_{sk}^*(\theta_k),$$

$$\Delta_k = \sum_{s=1}^6 \phi_{sk} \psi_{sk} = 1 + \frac{(\lambda_k^2 + 1)^2}{a_1 a_4} \left( \frac{a_3 a_5}{(\lambda_k^2 + a_2)^2} + 1 \right). \tag{14}$$

$\lambda_k$  is the natural frequency of derived equations.  $\bar{F}_1 = 0$ ,  $\bar{F}_2 = F_1$ ,  $\bar{F}_3 = 0$ ,  $\bar{F}_4 = F_2$ ,  $\bar{F}_5 = 0$ , and  $\bar{F}_6 = F_3$ . The basic solutions  $\phi_{sk}$ ,  $\phi_{sk}^*$ ,  $\psi_{sk}$ , and  $\psi_{sk}^*$  of derived equations and conjugate equations are obtained according to system (10),  $s = 1, 2, 3, 4, 5, 6$ ,  $k = 1, 2, 3$ .

Given that the rivulet vibrates mainly with the frequency of cable,  $F_0 \operatorname{sgn}(x_6)$  which is in system (8) is related to  $x_6$ , described as

$$\begin{aligned} x_6 &= A_1 \phi_{61} + A_2 \phi_{62} + A_3 \phi_{63} \approx A_1 \phi_{61} \\ &= \left( \frac{A_1 \lambda_1 (\lambda_1^2 + a_1)}{a_2} \right) \sin(\lambda_1 t), \end{aligned} \tag{15}$$

making  $x_6 = 0$  can ascertain the interval of the symbolic function. Thus  $\alpha_1 = \pi$ ,  $\alpha_2 = 2\pi$ . The last average equations can be written as

$$\begin{aligned} \frac{dA_k}{dt} &= \frac{\varepsilon}{2\pi \Delta_k} \left( \int_0^{2\pi} \sum_{s=1}^6 \bar{F}_s \psi_{sk}(\theta_k) d\theta_k \right) \\ &+ \frac{\varepsilon}{2\pi \Delta_k} \left( \int_0^{\alpha_1} \mu_0 F_0 \psi_{6k}(\theta_k) d\theta_k \right. \\ &\quad \left. - \int_{\alpha_1}^{\alpha_2} \mu_0 F_0 \psi_{6k}(\theta_k) d\theta_k \right), \end{aligned}$$

$$\begin{aligned} \frac{d\theta_k}{dt} = & \lambda_k - \frac{\varepsilon}{2\pi\Delta_k\gamma_k} \left( \int_0^{2\pi} \sum_{s=1}^6 \bar{F}_s \psi_{sk}^*(\theta_k) d\theta_k \right) \\ & - \frac{\varepsilon}{2\pi\Delta_k\gamma_k} \left( \int_0^{\alpha_1} \mu_0 F_0 \psi_{6k}^*(\theta_k) d\theta_k \right. \\ & \left. - \int_{\alpha_1}^{\alpha_2} \mu_0 F_0 \psi_{6k}^*(\theta_k) d\theta_k \right). \end{aligned} \quad (16)$$

Make

$$\frac{dA_1}{dt} = \frac{dA_2}{dt} = \frac{dA_3}{dt} = 0, \quad (17)$$

then

$$\begin{aligned} A_k &= A_{k0}, \\ \theta_k &= \varepsilon \frac{d\theta_k}{dt} (A_{k0}) t + \vartheta_k. \end{aligned} \quad (18)$$

$\vartheta_k$  is arbitrary constant; the steady state solutions are obtained by substituting (18) into (12)

$$x_s = \sum_{k=1}^3 A_{k0} \phi_{sk} \left( \left( \lambda_k + \varepsilon \frac{d\theta_k}{dt} (A_{k0}) \right) t + \vartheta_k \right). \quad (19)$$

## 4. Results Analysis

Parameters are selected as follows [20]:  $M = 64.8 \text{ kg/m}$ ,  $L = 110.5 \text{ m}$ ,  $R = 0.051275 \text{ m}$ ,  $T = 4.9 \times 10^6 \text{ N}$ ,  $A = 8.26 \times 10^{-3} \text{ m}^2$ ,  $E = 2.10 \times 10^{11} \text{ Pa}$ ,  $\alpha = 30^\circ$ ,  $\beta = 35^\circ$ ,  $\zeta_1 = 0.1\%$ ,  $\zeta_2 = 0.1\%$ ,  $\zeta_r = 0.0008 \text{ Ns/m}^2$ ,  $U_0 = 8 \text{ m/s}$ ,  $m = 0.16 \text{ kg/m}$ , and  $F_0$  is 10% of rivulet's mass per unit length.

**4.1. Numerical Solutions.** Figure 2 shows the numerical solutions of inclined cable vibration calculated from system (8) utilizing Matlab. The full line in Figure 2(a) is the time-history of in-plane vibration while the dotted line represents the out-of-plane vibration of the cable. The in-plane amplitude is about 4 times as that of out-of-plane vibration and they have the same phase. The time-history of the displacement response of the rivulet is presented in Figure 2(b). The moving rivulet vibrates at its equilibrium position. Note that, the vibration is not exhibited to be harmonic and there is not one frequency component. Figure 3 provides the vibration frequencies of in-plane and rivulet vibration. Cable vibrates at its natural frequency which is equal to 1.25 Hz as shown in the Figure 3(a). However, the frequency components of rivulet vibration are more complex. As shown in Figure 3(b), its primary frequency is the same as the natural frequency of cable; in addition, some higher order frequencies also exist in its vibration.

**4.2. The Comparison between Analytic and Numerical Solutions.** Figure 4 represents the analytic solutions together with the numerical results. The  $x$ -coordinate is the mean wind velocity  $U_0$  and the  $y$ -coordinate is the maximum displacement response amplitude of the in-plane, out-of-plane, and rivulet vibration, respectively. Analytic solution

is a smooth curve, describing the trend of the amplitude more directly and visually. Numerical solutions are several discrete points. The amplitudes of in-plane, out-of-plane, and rivulet vibration present a directly proportional relationship. The response curves also confirm that rain-wind-induced inclined cable vibration is a kind of restricted amplitude vibration rather than galloping. The analytic results are in good agreement with the numerical results. Thus, the validity of the approximately analytic method is proved.

**4.3. Analysis of Equilibrium Position of Rivulet.** The correspondences among the equilibrium position of rivulet, mean wind velocity, and rivulet mass are calculated from (6) and shown in Figure 5(a). The equilibrium position of rivulet is determined by mean wind velocity with certain rivulet mass. The effective wind velocity is around 1 m/s~24 m/s. Greater rivulet mass needs larger mean wind velocity to form on the surface of the inclined cable. Keeping the other parameters invariant, the effects of rivulet mass on the cable vibration subjected to variational mean wind velocity are presented in Figure 5(b). Greater rivulet mass on the surface of inclined cable will cause stronger oscillation. The impact of the equilibrium position of rivulet on the inclined cable is investigated and plotted in Figure 5(c). It can be perceived that the amplitude is up to the maximum when the equilibrium position of rivulet is around  $48^\circ$  and almost irrelevant to the rivulet mass. It confirms that the presence of rivulet at certain positions on the surface of inclined cable is one of the trigger that stimulate the inclined cable to vibrate.

**4.4. Nonlinear Dynamic Analysis.** The nonlinear dynamic behavior of cable reflected by parameters is given in Figure 6. The effect of mean wind velocity on the cable is presented in Figure 6(a), in which the full line is stable solution and the dotted line represents unstable solution. The figure illustrates that the mean wind velocity modify the number of the solutions. Two stable solutions appear at the mean wind velocity range from 7 m/s to 8.7 m/s. Figure 6(b) describes the nonlinear response curve of Coulomb damping force  $F_0$  acting on the cable amplitude subjected to various mean wind velocities. When mean wind velocity  $U_0$  is selected as 8 m/s, two stable solutions occur for  $F_0$  is less than 15%. As  $F_0$  increases, the amplitude of inclined cable first arises along the smaller branch of the stable solution and it will not jump until  $F_0$  reaches 15%. Once  $F_0$  increases to 15%, the smaller branch of amplitude will be substituted by the larger branch. The jump phenomena will also exist while  $F_0$  is about 9% for  $U_0$  is 7 m/s. The variance of  $F_0$  will make no change to the number of solution while the mean wind velocity is 6 m/s, where the system has only one stable solution and no jump phenomena occurs. Similarly, the response curve of damping ratio acting on the inclined cable depicts the nonlinear behavior of the system (Figure 6(c)). Multiple solutions lie in the certain range of  $\zeta_v$ , when  $U_0$  is beyond its critical mean wind velocity 7 m/s; otherwise, unique solution is obtained irrelevant to the damping ratio.

The relation curves of amplitude and the span length of cable  $L$  are obtained in Figure 6(d). It also illustrates

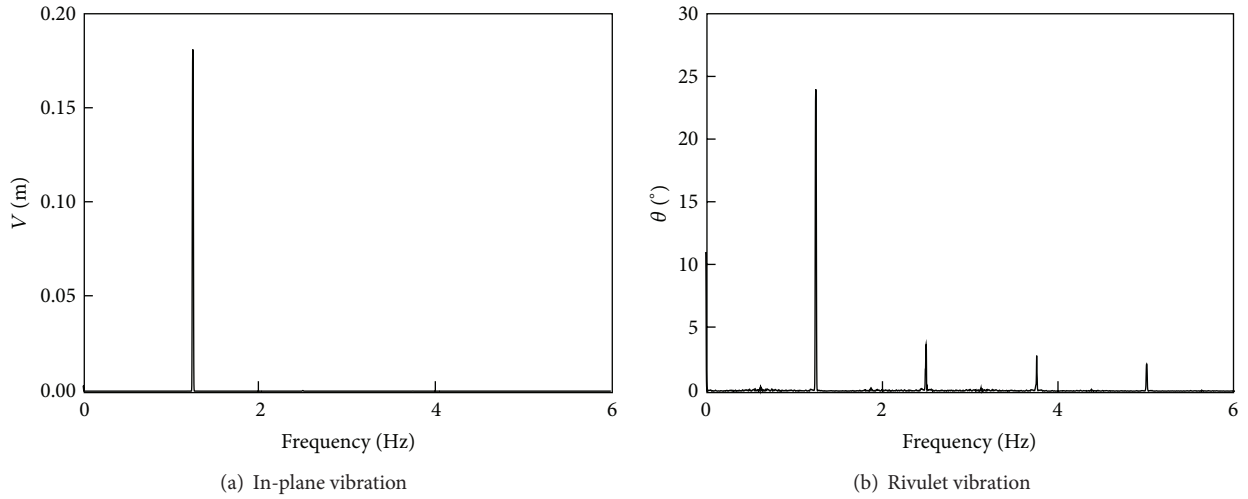


FIGURE 3: Vibration frequencies.

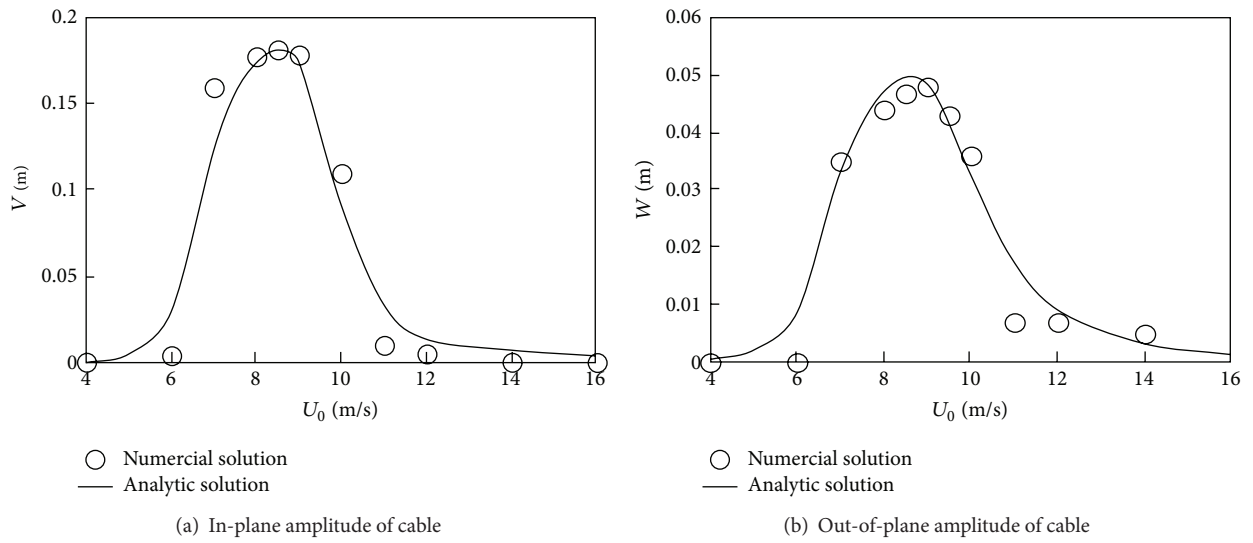


FIGURE 4: Comparison diagram of analytic and numerical solutions.

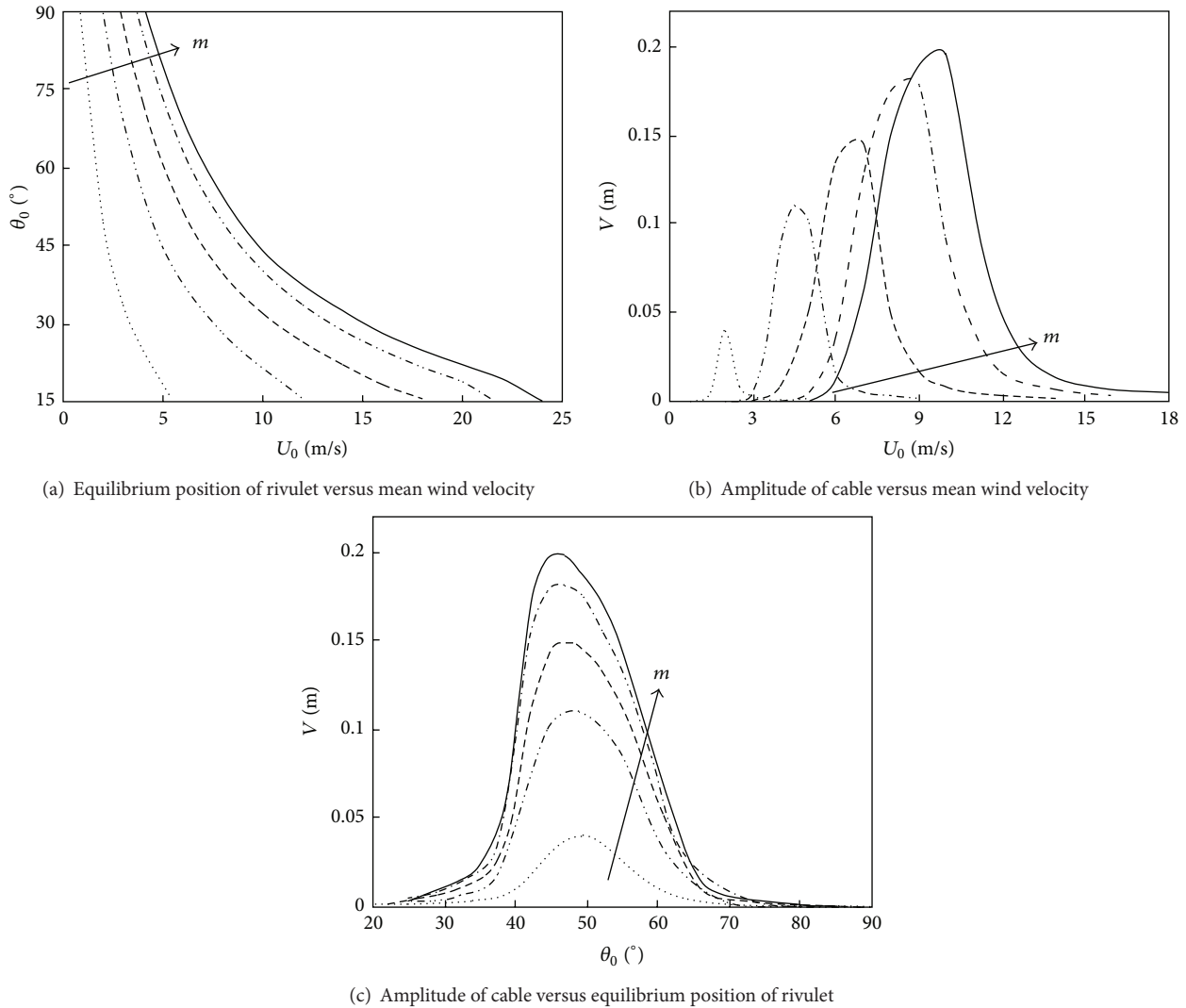


FIGURE 5: The correspondences between the equilibrium position of rivulet and mean wind velocity with a certain rivulet mass. Arrows indicate the growing direction of  $m$  ( $m = 0.01, 0.05, 0.1, 0.16, 0.2$ ).

that the mean wind velocity modified the stability of the inclined cable. When the mean wind velocity is selected as 7 m/s or 8 m/s, the amplitude will jump to a solution of higher branch as the span length of lengthens. However, the mean wind velocity of 6 m/s will not cause the modification of the number of the solutions but only a slight increase. Figure 6(e) shows the response curve of cable amplitude and initial tension  $T$ . Similarly, the mean wind velocity of 7 m/s and 8 m/s will cause cable amplitude to increase drastically while the lower wind velocity acting on the cable makes little sense to the variance of the initial tension.

## 5. Conclusions

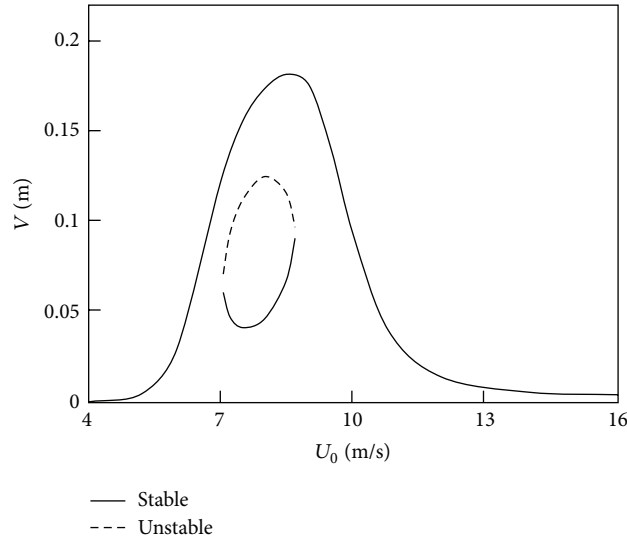
The continuum model of inclined cable subjected to wind with moving rivulet on its surface is established considering the equilibrium position of the rivulet. The Galerkin and average methods are adopted to analyze the cable system

analytically. The correspondence between mean wind velocity and the equilibrium position of the rivulet is ascertained considered the different rivulet mass. The equilibrium position of the rivulet is proved to be one of the major roles in determining the maximum amplitude of the oscillating cable.

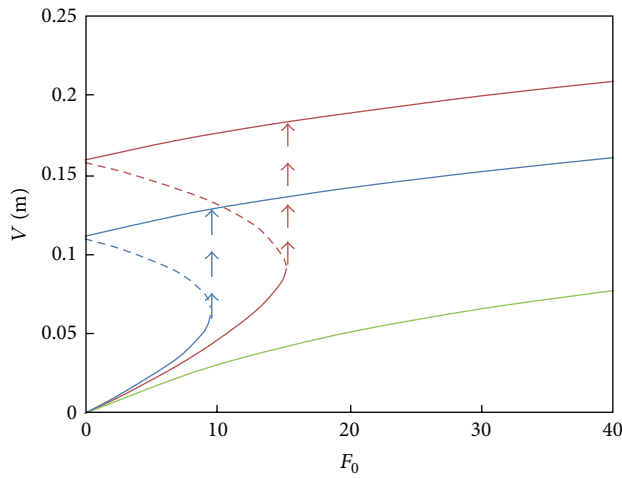
The nonlinear dynamic behavior of the rain-wind-induced cable vibration is then investigated considering the continuous change of parameters including mean wind velocity, Coulomb damping force, damping ratio, the span length, and the initial tension of the inclined cable. Mean wind velocity is observed to be a significant factor in jump phenomena, which is discovered in the range of multiple solutions.

## Acknowledgments

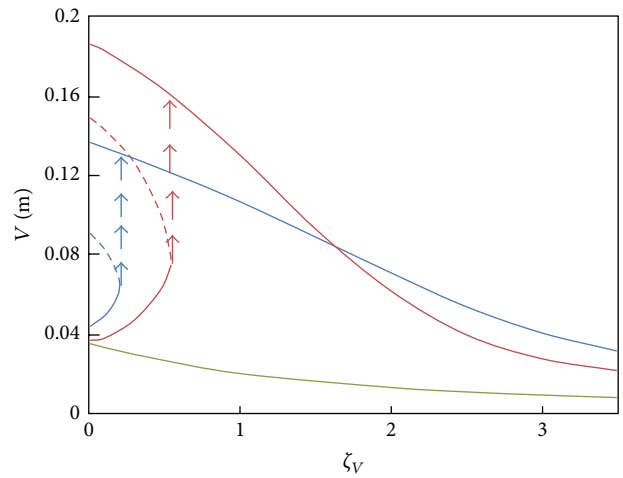
The authors wish to express their special gratitude to the reviewers and the editor for their valuable comments and



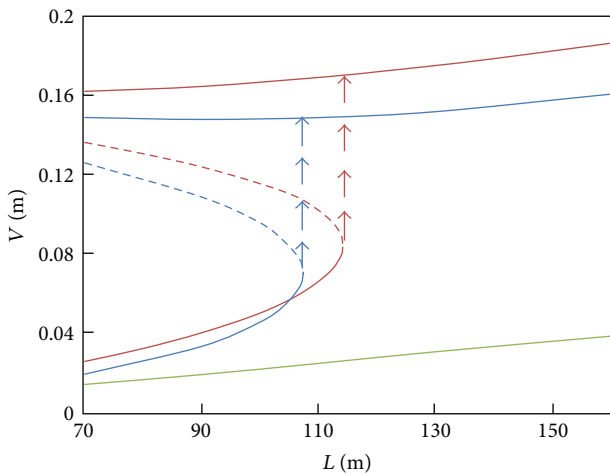
(a) Amplitude of cable versus mean wind velocity



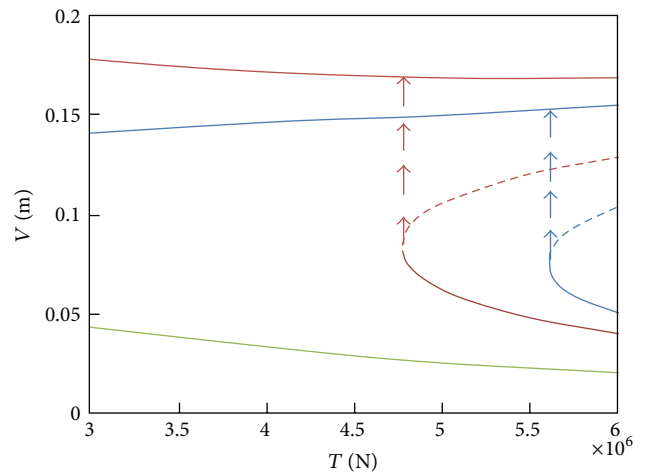
(b) Amplitude of cable versus Coulomb damping force  $F_0$



(c) Amplitude of cable versus damping ratio  $\zeta_v$



(d) Amplitude of cable versus the span length  $L$



(e) Amplitude of cable versus the initial tension  $T$

FIGURE 6: The nonlinear response curve with different parameters.

suggestions that led to a truly significant improvement of the paper. This work was supported by the National Natural Science Foundation of China (no. 51009107), Tianjin Natural Science Foundation (no. 13JCQNJC0420-0), and Key Project of Tianjin Natural Science Foundation (no. 13JCZDJC27100).

## References

- [1] M. Ferrara, F. Munteanu, C. Udriște, and D. Zugrăvescu, "Controllability of a nonholonomic macroeconomic system," *Journal of Optimization Theory and Applications*, vol. 154, no. 3, pp. 1036–1054, 2012.
- [2] C. Udriste and M. Ferrara, "Multitime models of optimal growth," *WSEAS Transactions on Mathematics*, vol. 7, no. 1, pp. 51–55, 2008.
- [3] Q.-C. Zhang, W.-Y. Li, and W. Wang, "Static bifurcation of rain-wind-induced vibration of stay cable," *Acta Physica Sinica*, vol. 59, no. 2, pp. 729–734, 2010.
- [4] A. H. Nayfeh, H. N. Arafat, C.-M. Chin, and W. Lacarbonara, "Multimode interactions in suspended cables," *Journal of Vibration and Control*, vol. 8, no. 3, pp. 337–387, 2002.
- [5] L. Wang and Y. Zhao, "Nonlinear interactions and chaotic dynamics of suspended cables with three-to-one internal resonances," *International Journal of Solids and Structures*, vol. 43, no. 25–26, pp. 7800–7819, 2006.
- [6] A. Luongo and G. Piccardo, "A continuous approach to the aeroelastic stability of suspended cables in 1 : 2 internal resonance," *Journal of Vibration and Control*, vol. 14, no. 1–2, pp. 135–157, 2008.
- [7] H. Chen and Q. Xu, "Bifurcations and chaos of an inclined cable," *Nonlinear Dynamics*, vol. 57, no. 1–2, pp. 37–55, 2009.
- [8] A. Luongo and D. Zulli, "Dynamic instability of inclined cables under combined wind flow and support motion," *Nonlinear Dynamics*, vol. 67, no. 1, pp. 71–87, 2012.
- [9] Y. Hikami and N. Shiraishi, "Rain-wind induced vibrations of cables stayed bridges," *Journal of Wind Engineering and Industrial Aerodynamics*, vol. 29, no. 1–3, pp. 409–418, 1988.
- [10] H. Yamaguchi, "Analytical study on growth mechanism of rain vibration of cables," *Journal of Wind Engineering and Industrial Aerodynamics*, vol. 33, no. 1–2, pp. 73–80, 1990.
- [11] M. Matsumoto, T. Saitoh, M. Kitazawa, H. Shirato, and T. Nishizaki, "Response characteristics of rain-wind induced vibration of stay-cables of cable-stayed bridges," *Journal of Wind Engineering and Industrial Aerodynamics*, vol. 57, no. 2–3, pp. 323–333, 1995.
- [12] M. Matsumoto, T. Yagi, M. Goto, and S. Sakai, "Rain-wind-induced vibration of inclined cables at limited high reduced wind velocity region," *Journal of Wind Engineering and Industrial Aerodynamics*, vol. 91, no. 1–2, pp. 1–12, 2003.
- [13] A. Bosdogianni and D. Olivari, "Wind-and rain-induced oscillations of cables of stayed bridges," *Journal of Wind Engineering and Industrial Aerodynamics*, vol. 64, no. 2–3, pp. 171–185, 1996.
- [14] M. Gu, X. Q. Du, and S. Y. Li, "Experimental and theoretical simulations on wind-rain-induced vibration of 3-D rigid stay cables," *Journal of Sound and Vibration*, vol. 320, no. 1–2, pp. 184–200, 2009.
- [15] L. Wang and Y. L. Xu, "Wind-rain-induced vibration of cable: an analytical model (1)," *International Journal of Solids and Structures*, vol. 40, no. 5, pp. 1265–1280, 2003.
- [16] Y. L. Xu and L. Y. Wang, "Analytical study of wind-rain-induced cable vibration: SDOF model," *Journal of Wind Engineering and Industrial Aerodynamics*, vol. 91, no. 1–2, pp. 27–40, 2003.
- [17] K. Wilde and W. Witkowski, "Simple model of rain-wind-induced vibrations of stayed cables," *Journal of Wind Engineering and Industrial Aerodynamics*, vol. 91, no. 7, pp. 873–891, 2003.
- [18] M. Gu, "On wind-rain induced vibration of cables of cable-stayed bridges based on quasi-steady assumption," *Journal of Wind Engineering and Industrial Aerodynamics*, vol. 97, no. 7–8, pp. 381–391, 2009.
- [19] E. H. Zhang, X. J. Liu, and S. X. Zhang, "Research on the factors of 3-D model of the rain-wind induced vibration of cable," *Engineering Mechanics*, vol. 29, no. 12, pp. 241–247, 2012.
- [20] J. L. Lilien and A. P. da Costa, "Vibration amplitudes caused by parametric excitation of cable stayed structures," *Journal of Sound and Vibration*, vol. 174, no. 1, pp. 69–90, 1994.